On the role of bank storage in attenuating lowland river floods

Gadadhara de Figueiredo FERRAZ[1,3], Tamás KRÁMER[2]

[1] Budapest University of Technology and Economics, Department of Hydraulic and Water Resources Engineering, Budapest, Hungary, 1521 Budapest, Pf. 91. (email: gadadhara.ferraz@emk.bme.hu)
[2] Budapest University of Technology and Economics, Department of Hydraulic and Water Resources Engineering, Budapest, Hungary, 1521 Budapest, Pf. 91. (email: kramer.tamas@emk.bme.hu)
[3] Corresponding author: gadadhara.ferraz@emk.bme.hu

DOI: 10.59258/hk.24054

Abstract

Overbank river floods generate a positive hydraulic gradient toward adjacent aquifers, while floodplain soils become saturated through vertical infiltration during the overbank phase of the flood. These processes contribute to temporary water storage and attenuate flood waves, yet their role in flood dynamics remains unrepresented or only partially represented in many models of river hydraulics. Here, we quantify river-aquifer exchange and evaluate the contribution of bank storage to flood attenuation at the scale of the Danube and Tisza Rivers in Hungary using a mechanistic model. We developed a coupled 1D surface water–2D groundwater model to simulate 100-year flood events in an idealised, prismatic geometry. Results, integrated over a 50 km reach, indicate that bank storage can account for 26–37% of the total (surface+bank) storage and can reduce peak flow by 0.7–0.8 percentage points in addition to the attenuation by surface storage. This translates to an average peak water level reduction of about 4 cm. The attenuation effect was most pronounced in systems with high soil hydraulic conductivity. Despite its role in mitigating flood risk, bank storage is frequently simplified to a conceptual level or omitted altogether in hydraulic river models. Since surface flow roughness parameters are routinely calibrated primarily against peak water levels, this omission is partially offset – even without identifying the source of error. However, compensating for the lack of groundwater storage within the timescale of surface storage is not only imperfect but also leads to inaccuracies when extrapolated to floods significantly larger than previously observed ones. Our findings underscore the benefits of integrating groundwater-surface water interactions into flood modelling to improve flood forecasts and risk assessments.

Keywords

Flood attenuation, bank storage, groundwater-surface water interaction, infiltration.

A felszín alatti tározódás szerepe a síkvidéki folyók árhullámainak csillapításában

Kivonat

Egy áradó folyó a nyomásgradiens révén szivárgást kelt a talajvíztartó irányába, és ezzel egy időben a partok szintjét meghaladó vízállások idején a hullámtér talaja a beszivárgás révén felülről is telítődik. A felszín alatti tározódás az árvizeknek a nagyvízi mederben való tározódásán felül érvényesül és ezáltal fokozza az árhullámok csillapítását, ennek ellenére leírása sok felszíni áramlástani modellből mégis hiányzik, vagy csak részleges. Jelen tanulmányban egy mechanisztikus modellel számszerűsítjük a folyó és a talajvíztartó közötti vízcserét a Duna és a Tisza hazai léptékében, valamint értékeljük a felszín alatti tározódás hozzájárulását az árvízcsillapításhoz. A szimulációkhoz egy egymással összekapcsolt 1D felszíni és 2D felszín alatti hidraulikai modellt fejlesztettünk ki, és 100 éves árvizek levonulását vizsgáltuk idealizált, prizmatikus geometriában. Egy 50 km hosszú folyószakaszra integrált eredményeink azt mutatják, hogy a felszín alatti tározódás a teljes (felszíni és felszín alatti) tározódásnak 26–37%-át teheti ki, és a felszíni tározódás által biztosított csillapításon felül további 0,7–0,8 százalékponttal csökkentheti a csúcsvízhozamot. Ez átlagosan körülbelül 4 cm-es csökkenést jelent a tetőző vízszintekben. A csillapító hatás a jó vízvezetőképességű talajok feltételezésével a legjelentősebb. Annak ellenére, hogy a felszín alatti tározódás számottevő szerepet játszik az árvízi kockázat mérséklésében, a felszíni áramlástani modellekben gyakran konceptuális szintre leegyszerűsítik vagy teljesen figyelmen kívül hagyják. Mivel a felszíni lefolyás simasági együtthatóit rutinszerűen elsősorban a folyó tetőző vízszintjein keresztül kalibrálják, ezért az elhanyagolás – a hibaforrás ismerete nélkül is – részben kompenzálódik. A talajvíz-tározódás hiányának a felszíni tározódás időskáláján való kompenzálása azonban nemcsak tökéletlen, de a múltbeli árvizeknél jóval nagyobbakra kiterjesztve pontatlan is. Eredményeink rávilágítanak arra, hogy az árvízi előrejelzések és kockázatértékelések javításához a modellezésbe érdemes bevonni a felszín alatti vizekkel való kölcsönhatást.

Kulcsszavak

Árhullám-csillapítás, parti tározás, felszín alatti és felszíni vizek kölcsönhatása, beszivárgás.

INTRODUCTION

River floodplains are essential for some hydrological and ecological processes, particularly during extreme flood events. They act as natural buffers, regulating runoff, storing excess water, and supporting essential biogeochemical cycles that mitigate nutrient and pollutant concentrations (*Krause et al. 2007*). Effective floodplain management requires understanding surface water–groundwater interactions and the connectivity between riverine and aquatic habitats, extending beyond in-channel processes to the active floodplain (*Sophocleous 2002*).

Direct field observations provide important insights into river–aquifer exchange processes during flood events. Observational studies have shown that groundwater levels in floodplain aquifers respond rapidly to changes in river stage, indicating strong hydraulic connectivity between rivers and adjacent aquifers. For example, *Li et al. (2017)* investigated groundwater dynamics in the floodplain wetlands of Poyang Lake, China, and found that floodplain groundwater is strongly influenced by lake water levels. Their results indicate that lake water recharges the floodplain aquifer during periods of high lake levels in spring and summer, whereas groundwater stored within the floodplain may discharge back to the lake during periods of low water levels, highlighting the bidirectional nature of lake–groundwater interactions. Similarly, *Ubell (1964)* analysed groundwater level profiles along a 30 km reach of the Danube in Hungary and estimated a mean infiltration of approximately 0.3 $m^3 s^{-1} km^{-1}$ during a flood event with a peak discharge of 5500 $m^3 s^{-1}$. However, direct measurements of river–aquifer interaction during extreme floods remain limited, and modelling approaches are therefore essential to quantify the magnitude and impacts of such exchanges (*Liang et al. 2018*).

Numerical modelling studies have therefore become an important tool to quantify river–aquifer interactions and their impact on flood dynamics. Early work by *Pinder and Sauer (1971)* and *Zitta and Wiggert (1971)* pioneered the coupling of one-dimensional (1D) unsteady open-channel flow with two-dimensional horizontal (2DH) groundwater flow to assess bank storage effects on the flood hydrograph. Subsequent modelling studies have further explored the dynamics of river–aquifer exchange and groundwater response to flood waves (*Weng et al. 2003, Vivoni et al. 2006, Derx et al. 2010, Liang et al. 2018*). More recently, integrated surface water–groundwater models have enabled the coupling of river hydraulics with variably saturated groundwater flow, allowing detailed simulation of infiltration processes and subsurface flow dynamics (*Shuai et al. 2017, Hong et al. 2020, Nguyen et al. 2025*). Integrating surface water–groundwater interactions into flood inundation models enhances river flow predictions and flood response assessments, leading to more reliable forecasts (*Szilagyi 2004, Saksena et al. 2019*). Process-based river models primarily rely on calibrated roughness coefficients to route flood waves. Operational flood forecasting systems and most 1D/2D hydraulic models omit explicit river–aquifer bank-storage exchange; although coupling to variably saturated groundwater models is technically feasible and has been demonstrated in several research studies (*Shuai et al. 2017, Hong et al. 2020, Nguyen et al. 2025*), it is still rarely implemented in operational forecasting models. The absence of a bank storage mechanism may be partly compensated for by modifying the roughness coefficients, but this often leads to significant inaccuracies in flood estimates, overpredicting river discharge during flood events (*Saksena et al. 2019*).

Several studies have combined field observations with numerical modelling to better constrain river–aquifer interactions during flood events. These studies typically use groundwater monitoring data to calibrate or validate numerical models of bank storage and groundwater response (*Vivoni et al. 2006, Liang et al. 2018*). Such combined approaches have demonstrated that rapid river stage fluctuations during large flood events can induce substantial water, sediment, and nutrient exchanges across the river–aquifer interface (*Bernard-Jannin et al. 2016*). *Bernard-Jannin et al. (2016)* combined field observations with numerical modelling to quantify both lateral riverbank infiltration and vertical infiltration across inundated floodplains during flood events. Their results indicate that overbank flow across the floodplain surface can dominate river–aquifer exchanges during long-duration floods, contributing up to 88% of total infiltration. However, many studies still focus primarily on lateral infiltration through riverbanks under in-bank flow conditions, while the contribution of vertical infiltration across inundated floodplains remains less explored.

These limitations highlight important knowledge gaps regarding the relative importance of horizontal riverbank infiltration and vertical infiltration across inundated floodplains, particularly for large lowland rivers during extreme floods. Addressing these gaps requires modelling approaches capable of isolating the influence of flood duration, river geometry, and soil hydraulic properties on river–aquifer exchange processes.

This study aims to investigate the relationships between key parameters – flood duration, channel geometry, and soil properties – and their influence on infiltration flows, bank storage, and flood attenuation. River–aquifer water exchange can be divided into (predominantly) horizontal and vertical infiltration, driven by variations in river stage. Horizontal infiltration across the riverbed induces the lateral propagation of a groundwater wave as surface water levels rise, while vertical infiltration penetrates into the unsaturated floodplain soil when floodwaters exceed bank elevations. To explore these mechanisms, we employ a coupled 1D surface water–2DH groundwater model for a fully penetrating river within an aquifer, using Darcy's law for exchange flow calculations (similar to the MODFLOW RIV package). Since the parameters determining the impact of infiltration vary from river to river, or from reach to reach, we focus here on the two largest rivers in Hungary, which have large, leveed floodplains of high aggregate flood risk. We apply this model to two idealised reaches: the lower reach of the Danube River and the middle reach of the Tisza River, the Danube's tributary, using a hypothetical 100-year return period flood hydrograph.

MATERIALS AND METHODS

A process-based model combining the 1D Saint-Venant equations with the 2DH groundwater flow equations derived from Darcy's law and mass conservation was used to simulate river flood propagation and its interaction with groundwater. Exchange fluxes from the river to the groundwater, driven by changes in river levels, are divided into horizontal and vertical components. In this study, we define vertical fluxes (f_V) as those occurring across the floodplain, while horizontal fluxes (f_H) are those that occur across the riverbed. Bank storage is also split according to the origin of the influx: BS_V represents the infiltrated volume from vertical fluxes, while BS_H represents the infiltrated volume from horizontal fluxes. When river water levels (h_R) rise above the riverbanks (H), water simultaneously flows into the aquifer vertically (f_V) through the floodplain and horizontally (f_H) through the riverbed. Consequently, the groundwater head (h_A) rises.

The geometry of the modelled reach is assumed to be prismatic, meaning that the cross-sectional shape and dimensions remain constant along the longitudinal direction, and the channel is characterized by a uniform bed slope. Under this assumption, no longitudinal variations in channel width, depth, or floodplain extent are considered within the modelled reach. The cross-section of the river is approximated as a combination of two rectangular sections: a main channel with width b and depth z, and an active floodplain of width b_{f_L} and b_{f_R} on the left and right banks, respectively, between the banks of the main channel and levees or higher terrain. *Figure 1* illustrates the generalised model configuration on which the physical processes are formulated.

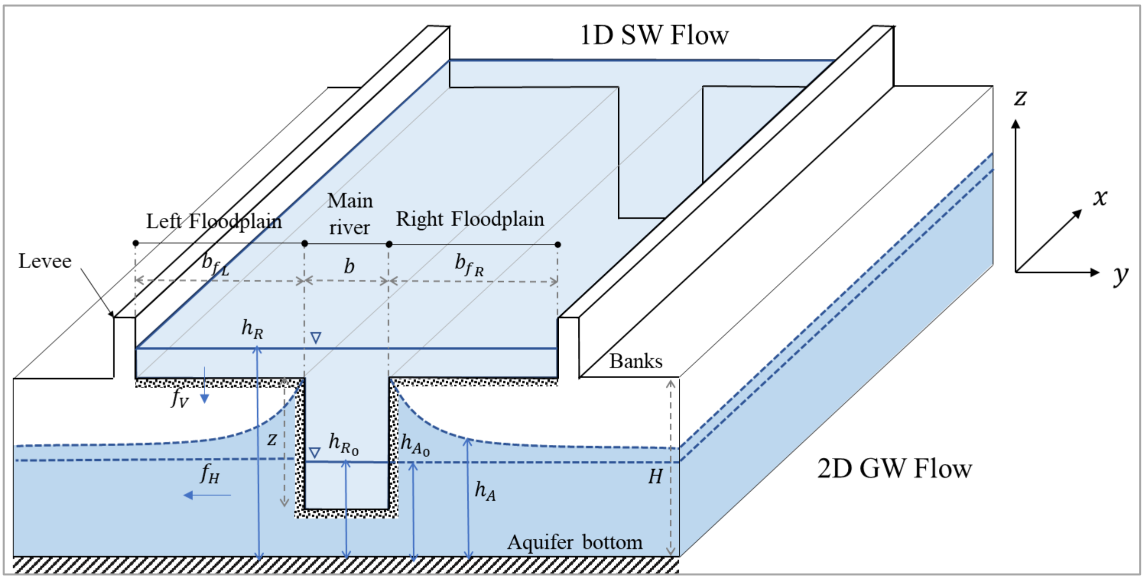

Figure 1. Model configuration in a cartesian coordinate system: 1D channel flow in the x direction, 2DH groundwater flow in the x–y direction, and 1D vertical infiltration

1. ábra. Modellfelépítés Descartes-i koordinátarendszerben: 1D felszíni lefolyás az x irányban, 2DH talajvízmozgás az x–y síkban és 1D függőleges beszivárgás

The groundwater module accounts for both confined and unconfined conditions depending on the position of the simulated groundwater head relative to the aquifer top. When the groundwater head is below the top of the aquifer, flow is treated as unconfined and storage is represented by the specific yield. When the groundwater head exceeds the aquifer top, the aquifer behaves as confined and storage is governed by the specific storage coefficient.

The model assumes a homogeneous and isotropic aquifer, hydraulically connected to the river, and an impermeable, horizontal base. The water level in the river and the piezometric head in the aquifer are measured from this base. The hydraulic connection between the river and the aquifer is represented through a riverbed and floodplain clogging layer with hydraulic properties distinct from those of the underlying aquifer, which controls the exchange flow between surface water and groundwater (*Brunner et al. 2009*).

The surface water domain boundaries were defined with sufficient extent to minimise any potential influence of downstream and lateral boundary conditions on flood attenuation or exchange flows within the analysed reach. The groundwater domain is bounded by no-flow conditions, except at the river-aquifer interface, where f_H (dimension: L/T) is imposed, governed by Darcy's law in proportion to the head difference between the river and the groundwater adjacent to the river. Similarly, f_V is imposed as a source term across the inundated floodplain and an equal-magnitude (but opposite) sink term in the groundwater domain. More specifically,

$$f_H = \frac{K_{rb}}{m_{rb}}(h_A - h_R), \qquad \text{and} \qquad f_V = \begin{cases} \frac{K_z}{m}[\max(h_A, H_b) - h_R] & \text{if } h_R > H_b \\ 0 & \text{otherwise,} \end{cases} \tag{1}$$

where K_{rb} and K_z are the hydraulic conductivities of the riverbed sediments and of the floodplain surface layer, respectively (dimension: L/T); h_R is the height of the river water surface above the aquifer bottom, calculated by the surface water model and uniform across the river section; h_A is the hydraulic head of the aquifer, calculated by the groundwater model and variable across the aquifer; m_{rb} and m are the thicknesses of the clogged interface layer in the riverbed and the floodplain, respectively (dimension: L); and H_b is the aquifer thickness (dimension: L).

Although natural aquifers may exhibit longitudinal hydraulic gradients parallel to the river, preliminary simulations were conducted using both a 1D and a fully 2D groundwater flow formulation to evaluate the influence of longitudinal groundwater flow. The results showed negligible differences between the two configurations, indicating that during flood events the dominant exchange processes are controlled by river–aquifer head gradients rather than regional longitudinal groundwater flow. Therefore, no-flow lateral boundaries were considered an appropriate simplification for the purposes of this study.

The methodology used here to calculate exchange flows is analogous to that used in the MODFLOW-2005 River Package (*Harbaugh 2005*). However, we developed our own finite-difference solver rather than using MODFLOW so that river flood propagation could be simulated more accurately with the full Saint-Venant equations, distinguishing between the Manning coefficient of the channel and that of the floodplain. The river domain is discretised into a sequence of equidistant cross-sections and the groundwater domain into a regular rectangular grid. The transverse gridlines of the groundwater domain overlap with the river cross-sections, but extend well beyond the levees. For each grid cell covering the active floodplain, a vertical flux is calculated.

Study area

We integrate bank storage and evaluate flood attenuation for two 50-km-long reaches, each approximating the mean geometry of the Lower Danube and the middle reach of the Tisza River in Hungary. At the inflow, a 100-year flood hydrograph was imposed, approximated separately for the two rivers. Soil hydraulic properties were kept constant over time.

The Lower Danube River in Hungary has a total floodplain width of approximately 1800 m, whereas the middle reach of the Tisza River features a slightly wider floodplain of about 2000 m. Both rivers have similar channel depths under banks (9.0 m for the Danube and 7.0 m for the Tisza), but the Danube's main channel is significantly wider (475 m compared to 180 m for the Tisza). Besides the geometry, the two rivers analysed also exhibit distinct flood hydrograph characteristics (*Figure 2*). The Danube has an overbank flood duration ($T_{overbank}$) of 15 days, reaching a peak discharge of 9850 m³/s on the 6th day after the start of overbank flood. The Tisza's flood extends for 80 days, with a peak flow of 2800 m³/s on day 40 after the beginning of the overbank flood.

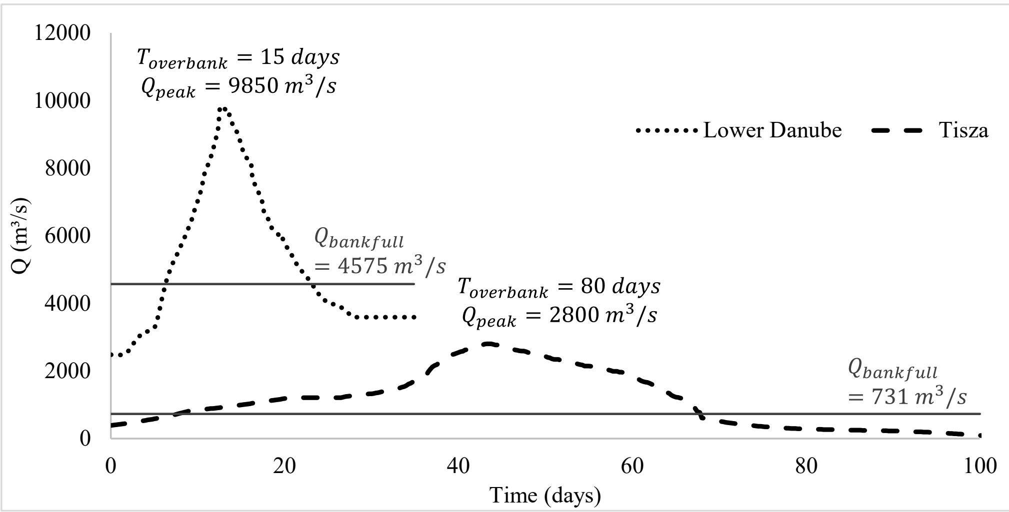

Figure 2. 100-year (HQ1%) flow hydrograph of the Lower Danube (dotted line) and the Tisza River (dashed line). Bankfull discharges are represented by solid lines for the Lower Danube and the Tisza. The vertical axis represents river flow Q (m³/s), while the horizontal axis shows time in days

2. ábra. A hazai Alsó-Duna (pontozott vonal) és a Közép-Tisza (szaggatott vonal) 100 éves visszatérési idejű (HQ1%) árhullámképe. A mederkitöltő vízhozamokat folytonos vonal jelöli az Alsó-Duna és a Tisza esetén. Függőleges tengely: Q vízhozam (m³/s), vízszintes tengely: idő (nap)

The hydraulic conductivity of the soil was varied by discretising the order of magnitude with three scenarios, SCN25 to SCN27 for the Danube River and SCN28 to SCN30 for the Tisza River, to address the spatial variability and uncertainty of soil hydraulic conductivity. The adopted conductivity values were not derived from direct field measurements within this study but were inferred from reported ranges in previous hydrogeological investigations of the region (*Ubell 1963, Kolencsik-Tóth and Kovács 2015, Murinkó and Bene 2017, Trásy et al. 2020, Wagner and Csoma 2022*). These studies describe the alluvial deposits surrounding the investigated rivers as predominantly sandy and gravelly aquifers. Based on these reported ranges, representative hydraulic conductivity values were selected and further adjusted during model calibration together with the Manning roughness coefficient.

Rather than representing a specific statistical distribution of measured values, the three scenarios were designed to capture plausible low-, medium-, and high-conductivity conditions within the range reported for similar alluvial environments. The upper conductivity scenario ($K_x = 500$ m/d; SCN27/30) represents a high-permeability gravel aquifer condition, characteristic of coarse alluvial deposits with strong river–aquifer connectivity, and was included to investigate the upper sensitivity range of infiltration and bank storage processes.

Table 1 summarises the data utilised in the model. For the Danube River, two reaches have been distinguished. The Lower Reach served for calibration and the analysis of the 100-year flood wave, whereas the Upper Reach was evaluated to validate the transferability of model parameters.

Table 1. Hydraulic parameters and their values used in the model for the analysed rivers.
1. táblázat. A vizsgált folyók modelljében használt hidraulikai paraméterek és értékeik

Parameter	Danube River (Lower Reach)	Danube River (Upper Reach)	Tisza River	Unit	Description
$\boldsymbol{b}$	475	574	180	m	Bottom width of the main channel
$\boldsymbol{z}$	9	7.5	7.0	m	Depth of the main channel
$\boldsymbol{S_0}$	7	7	2.5	cm/km	River slope
$\boldsymbol{n_m}$	0.033	0.033	0.03	s m$^{-1/3}$	Manning roughness of the main channel
$\boldsymbol{n_f}$	0.1	0.1	0.082	s m$^{-1/3}$	Manning roughness of the active floodplain
$\boldsymbol{b_f}$	1,800	240	2,000	m	Total width of the active floodplain
$\boldsymbol{K_{rb}/m_{rb}}$	0.15	0.15	0.15	d^{-1}	Riverbed leakance factor = ratio of riverbed hydraulic conductivity per thickness of the riverbed layer
$\boldsymbol{S_y}$	0.21	0.21	0.21	-	Specific yield for unconfined aquifer
$\boldsymbol{S_s}$	1×10^{-5}	1×10^{-5}	1×10^{-5}	m^{-1}	Specific storage when aquifer is fully saturated
$\boldsymbol{K_x = K_y}$	SCN25: 5 SCN26: 50 SCN27: 500	SCN25: 5 SCN26: 50 SCN27: 500	SCN28: 5 SCN29: 50 SCN30: 500	m d^{-1}	Horizontal hydraulic conductivity of the aquifer
$\boldsymbol{K_z}/m$	SCN25: 0.15 SCN26: 1.5 SCN27: 15	SCN25: 0.15 SCN26: 1.5 SCN27: 15	SCN28: 0.15 SCN29: 1.5 SCN30: 15	d^{-1}	Vertical leakance factor = ratio of floodplain vertical hydraulic conductivity per thickness of the floodplain surface layer
Q_{peak} (100-yr)	9,850	-	2,800	m^3 s^{-1}	Peak discharge during the 100-year flood hydrograph ($HQ_{1\%}$)
$T_{overbank}$ (100-yr)	16.75	-	60.25	d	Duration of overbank flooding during the 100-year event
Q_{peak} (2013)	9,080	9,346	-	m^3 s^{-1}	Peak discharge during the 2013 flood hydrograph
$T_{overbank}$ (2013)	16.0	15.5	-	d	Duration of overbank flooding during the 2013 event
$Q_{bankfull}$	4,575	4,522	731	m^3 s^{-1}	Bankfull discharge

The longitudinal slope was set to the mean slope of the actual river reaches.

Model calibration targeted three key variables: (1) the mean overbank depth (d), (2) the relative attenuation of peak discharge, expressed as $\Delta Q/Q_{peak} = \left[Q_{peak}(0) - Q_{peak}(L_x)\right]/Q_{peak}(0)$, where $Q_{peak}(0)$ is the river peak discharge at the inflow, and $Q_{peak}(L_x)$ is the river peak discharge at the longitudinal length from which attenuation is analysed, L_x, and (3) the average bank storage within the dry floodplain, defined as the area beyond the levees extending approximately 3 km inland. No groundwater data were available on the active floodplain (which is a routine limitation); therefore, calibration primarily focused on estimating bank storage within the dry floodplain (BS_{dry}).

The variables adjusted during calibration were the Manning roughness coefficient (n) of the river model and the vertical leakance factor, that is, the ratio of the floodplain vertical hydraulic conductivity of the soil to the thickness of the floodplain surface layer (K_z/m). The leakance factor of the riverbed was kept constant between scenarios because the observed variables were barely sensitive to it.

Uniform and river-specific Manning's n values were calibrated for the channel and floodplain using the 2013 flood of the Danube River over the 135 km Lower Danube reach between the river gauges of Dunaújváros and Mohács (rkm 1580-1446). The calibration targets were the mean overbank depth (d) and the relative attenuation of the peak discharge ($\Delta Q/Q_{peak}$). This approach was used to evaluate whether a simplified symmetric cross-section could represent the overall hydraulic behaviour of the actual irregular river sections, rather than to reproduce observations at individual gauge stations.

The floodplain geometry of this reach is highly variable, being relatively narrow along the upstream two-thirds and wider along the downstream third. Due to the nonlinear nature of the Saint–Venant equations, the prismatic model could not simultaneously reproduce both calibration indicators with exact agreement.

We validated the transferability of the model parameters to a distinct 47 km reach between the left-bank tributaries, the Váh (Vág) River and Hron (Garam) River, delimited by river gauges Iža and Esztergom (rkm 1764-1718.5), to which we refer here as the Upper Danube Reach. The reach was not extended beyond the tributaries to simplify the evaluation of flood peak attenuation. Except for the floodplain width, the character of the river and aquifer are similar to those of the Lower Danube Reach, so we transferred the Manning n values and the aquifer parameters unchanged and only updated the (still simplified) geometry of the river.

The floodplain in this reach is considerably narrower, which alters the relative contribution of vertical floodplain infiltration and horizontal riverbank infiltration processes. As a result, the simulated d and $\Delta Q/Q_{peak}$ show larger deviations from the reference values compared to the calibration reach. For the Lower Danube reach, simulated d ranges from 2.57 to 2.67 m compared to the target value of 3.0 m, while $\Delta Q/Q_{peak}$ ranges from 10.2% to 11.5% compared to the target value of 8.2%. For the Upper Danube reach, simulated $\Delta Q/Q_{peak}$ ranges from 0.9% to 1.1% compared to the reference value of 2.0% (*Table 2*). These differences indicate that the calibration compensates for the geometric variability of the Lower Danube floodplain and therefore performs less effectively when transferred to the more regular Upper Danube reach. However, because the objective of the model is to reproduce the order of magnitude of flood attenuation for idealised lowland river geometries rather than site-specific hydraulic conditions, we considered these deviations to be reasonable.

Table 2. Reference and simulated mean overbank depth (d) and flow attenuation ($\Delta Q/Q_{peak}$) over 135 km for the Lower Danube reach (used in the calibration), and over 47 km for the Upper Danube reach (used in the validation of parameter transferability), during the 2013 flood

2. táblázat. Referenciaként adott és szimulált átlagos hullámtéri vízmélység (d) és relatív vízhozam-csillapítás (ΔQ/Q_peak) a 2013-as árvíz idején; az Alsó-Duna 135 km-es szakaszán (kalibráció), valamint a Felső-Duna 47 km-es szakaszán (a paraméter-átvihetőség igazolása)

	Lower Danube (Calibration)				**Upper Danube (Validation)**			
	Target	**SCN25**	**SCN26**	**SCN27**	**Target**	**SCN25**	**SCN26**	**SCN27**
d (m)	**3.0**	2.67	2.66	2.57	**3**	4.43	4.41	4.41
$\boldsymbol{\Delta Q/Q_{peak}}$ (%)	**8.2**	10.3	10.2	11.5	**2.0**	0.9	1.1	1.0

For the groundwater model, the ratio of floodplain vertical hydraulic conductivity of the soil to the thickness of the floodplain surface layer was determined by targeting the bank storage under the dry floodplain (beyond the levees), as, for example, by *Ubell (1964).* Model results were compared with bank storage estimates derived from observed groundwater level data sourced from the General Water Directorate of Hungary.

Stations with a significant share of missing or erroneous data were excluded, resulting in a total of 21 valid groundwater stations on the left bank of the lower reach and 25 stations on the right bank of the upper reach for use in the final analysis. The wells are distributed along the study reaches at varying distances from the levee and river channel rather than along a single transect, and therefore represent groundwater responses across different locations of the dry floodplain.

These stations were all situated on the dry floodplain; the lack of data on the groundwater table or the saturation of the vadose zone under the active floodplain is the reason why total bank storage could not be estimated.

To evaluate groundwater response during the flood event from the measured gauge data, the maximum rise in groundwater level – from initial to peak stage – was plotted against the distance of each well from the levee (*Figure 3*). The levee serves as the boundary between the dry and wet floodplains. A logarithmic curve was fitted to the data, and a length-normalised bank storage under the dry floodplain (BS_{dry}) was estimated as the positive area under this lateral profile multiplied by a river length of 50 km.

For the Lower Danube Reach, the minimum distance between a groundwater well and the levee is 31 m, with an observed maximum groundwater rise of 2.86 m (average 0.65 m). For the Upper Danube Reach, these values are 54 m, 4.24 m, and 0.74 m, respectively. The distance over which the flood had a direct impact was about 2500 m in both reaches. The bank storage along the left dry floodplain was approximately 13 × 10^6 m³ (16 × 10^6 m³) over 50 km. For both reaches, we estimated that the total bank storage under the dry floodplain (BS_{dry}) was twice the one-sided value.

During calibration and validation, the numerical model was applied to the 2013 flood event of the Danube River, using three sets of hydraulic conductivity values representing plausible ranges for alluvial aquifers reported in the literature. Horizontal conductivities of 5, 50, and 500 m d^{-1} were tested, each paired with vertical leakance factors of 0.15, 1.5, and 15 d^{-1}, respectively. These parameter sets were used to explore the sensitivity of the simulated groundwater response and bank storage to hydraulic conductivity. The initial condition of the groundwater head was assumed to be in equilibrium with the surface water head.

As in the observational analysis, only the bank storage under the dry floodplain was calculated from the model results. *Table 3* presents both the observation-based bank storage estimates (derived from groundwater level data) and the simulated values. Considering that the modelled BS_{dry} varied by more than a factor of 16 between the bounding scenarios, BS_{dry} for the medium conductivity scenario (24×10^6 m^3) aligned well with the value derived from measurements (25×10^6 m^3). Model validation using the Upper Danube Reach yielded a measurement-based estimate of 32×10^6 m^3, compared to a result of 24×10^6 m^3 modelled with the medium K scenario. This is satisfactory evidence that the medium K scenario captures the order of magnitude of the mean conductivity for the Danube.

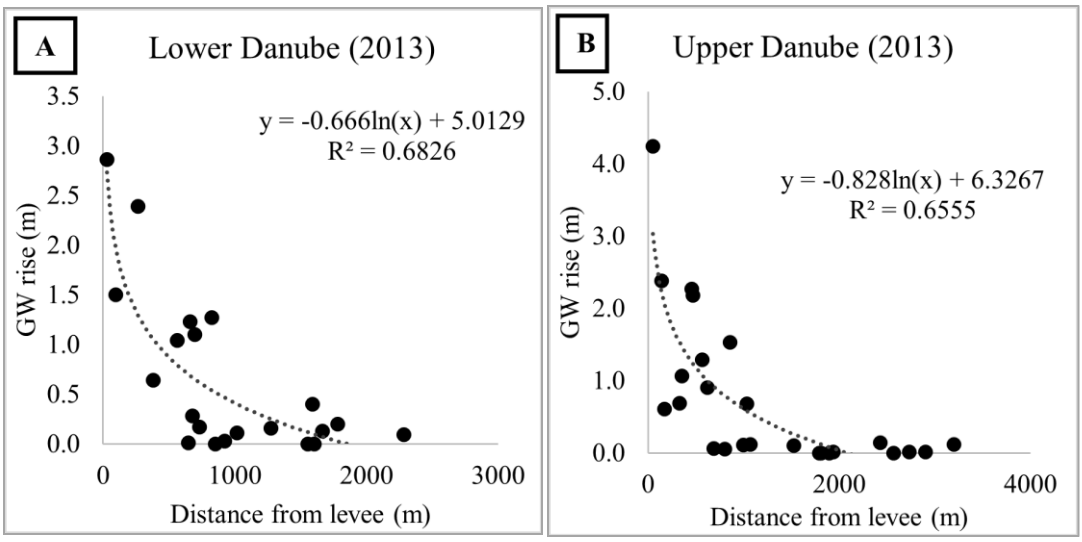

Figure 3. Observed maximum groundwater rise (y) during the 2013 Danube flood as a function of distance from the levee on the dry floodplain (x), for the lower (A) and the upper (B) Danube reach
(A logarithmic regression curve was fitted to the data)
3. ábra. Megfigyelt maximális talajvízszint-emelkedés (y) a 2013-as dunai árvíz idején a mentett oldali ártéren, az árvízvédelmi töltéstől mért távolság (x) függvényében, az alsó (A) és a felső (B) dunai szakaszra
(Az adatokra logaritmikus regressziós görbe lett illesztve)

Table 3. Simulated and measured bank storage under the dry floodplain (BS_{dry}, [10^6 m³]) on the left (Lower Danube) and right (Upper Danube) banks, during the 2013 flood. "Measured" bank storage was estimated from observed groundwater level data
3. táblázat. A szimulált és a mért felszín alatti tározódás összehasonlítása a mentett oldali ártér alatt (BS_{dry}, [10^6 m³]) a dunaszakaszok bal (Alsó-Duna) ill. jobb (Felső-Duna) partján, a 2013-as árvíz idején. A „mért" felszín alatti tározódást a megfigyelt talajvízszint-adatok alapján becsültük

Conductivity scenario	Lower Danube reach		Upper Danube reach	
	Numerical model	Measured	Numerical model	Measured
SCN25 (low K)	3	25	6	32
SCN26 (medium K)	24	25	24	32
SCN27 (high K)	80	25	43	32

The definition of the flood start introduces some uncertainty in the estimation of bank storage, particularly when antecedent water level variations precede the main flood wave. Since bank storage was estimated from the groundwater rise between the initial and peak stages, changes in the selected initial condition may influence the absolute storage values. However, the same flood period and initial conditions were used for both the observation-based estimates and the numerical simulations, ensuring consistency in the comparison between measured and modelled bank storage.

The Manning n values of the Tisza River were calibrated separately, as for the Lower Danube Reach, against maximum overbank depth and discharge peak attenuation. Results are not presented here. The hydraulic properties of the aquifer were transferred from the Danube River without recalibration or validation.

Groundwater calibration and validation were only performed for the Danube River. Although a dense groundwater monitoring network exists along the Middle Tisza River, preprocessing and interpretation of the groundwater time series were beyond the scope of the present study. Therefore, the Tisza results are presented as scenario-based sensitivity analyses, and no individual hydraulic conductivity scenario is interpreted as the best-fitting representation of field conditions.

In the following sections, we analyse how these characteristics influence exchange flows between rivers and aquifers, bank storage, and their contribution to flood attenuation for the Lower Danube Reach and the Tisza River, which differ markedly in flood magnitude, flood duration, and longitudinal slope. The Upper Danube Reach will not be analysed further.

RESULTS

To assess the effect of bank storage on the attenuation of flood peaks, we seek to determine the mean lateral exchange of water from the channel into adjacent aquifers (expressed as a volumetric flow per unit river length) and to evaluate how this exchange varies spatially over management-relevant scales. To this end, we averaged the instantaneous volumetric flow rates Q_V and Q_H at each model transect during the simulation period, excluding zero flows. Finally, to obtain a reach-scale metric, we averaged these volumetric flows over a 50 km reach.

This 50 km average length was chosen because it approximates typical levee-management units and is long enough to integrate cumulative attenuation effects while remaining short enough to align with operational planning. The resulting 50 km-averaged specific flow components, q_H and q_V, provide a meaningful indicator of bank-storage capacity that can be directly compared across the Hungarian reaches of the Danube River and Tisza River.

Regarding the bank storage volume, we first calculate the time evolution of the specific bank storage for each transect by integrating the specific infiltration flow rate over time for the entire duration of the flood hydrograph. For each transect, we then identify the maximum value of the specific bank storage, which we finally integrate over a 50 km reach, resulting in 50 km-averaged peak specific bank storage components BS_H and BS_V. Note that these capture bank storage under the entire floodplain, including the active and the dry floodplains.

Table 4 summarises the results for mean specific flow rates from the river and peak specific bank storage, both per river km, across the six different river scenarios analysed.

Table 4. Vertical and horizontal components, and total specific infiltration flow from the river into the aquifer (q_V, q_H, q_T), averaged over the simulation period of the 100-year flood. The associated maximum bank storage volumes (BS_V, BS_H, BS_T), for all scenarios. All variables are averaged/integrated over a 50 km river length
4. táblázat. A folyóból a talajvíztartóba irányuló fajlagos szivárgási vízhozam függőleges és vízszintes összetevői és ezek összege (q_V, q_H, q_T), a 100 éves árvíz szimulációs időszakára átlagolva. A táblázat tartalmazza a hozzájuk tartozó maximális felszín alatti tározott víztérfogatokat is (BS_V, BS_H, BS_T) minden változatra. Minden változó 50 km-es folyószakaszra átlagolva/integrálva értendő

Scenario	River	K_z/m [d^{-1}]	K_x [m/d]	Mean q_V [m³/s/km]	Mean q_H [m³/s/km]	Mean q_T [m³/s/km]	Max BS_V [10³ m³/km]	Max BS_H [10³ m³/km]	Max BS_T [10³ m³/km]
SCN25	Lower Danube	**0.15**	**5**	0.58	0.09	0.67	1,013	111	1,125
				(87%)	(13%)		(90%)	(10%)	
SCN26		**1.5**	**50**	0.81	0.16	0.97	1,419	181	1,600
				(84%)	(16%)		(89%)	(11%)	
SCN27		**15**	**500**	1.54	0.22	1.76	2,632	249	2,880
				(88%)	(13%)		(91%)	(9%)	
SCN28	Tisza	**0.15**	**5**	0.16	0.03	0.19	1,091	126	1,217
				(84%)	(16%)		(90%)	(10%)	
SCN29		**1.5**	**50**	0.25	0.04	0.29	1,742	173	1,915
				(86%)	(14%)		(91%)	(9%)	
SCN30		**15**	**500**	0.58	0.07	0.65	3,763	285	4,048
				(89%)	(11%)		(93%)	(7%)	

In both rivers, specific infiltration flows through the floodplain (q_V) were greater than those through the riverbed (q_H), contributing approximately 86% of the total specific infiltration flows, owing mainly to the large floodplain width. The bank storage volume originating from the vertical infiltration (BS_V) represents 91% of the total ($BS_V + BS_H$) for the Tisza River scenarios and 90% for the Danube River scenarios.

Exchange flows

River–aquifer exchange flows are driven by the hydraulic gradient between river water and groundwater levels, which is conceptually split into horizontal and vertical infiltration pathways. The total reach-integrated infiltration flow rate, obtained as the sum of vertical and horizontal flow rates ($Q_T = Q_H + Q_V$), has a sharper peak than the surface flow hydrograph.

Figure 4 presents the exchange flow hydrographs for the three hydraulic conductivity scenarios of the Danube River. As expected, higher hydraulic conduc-tivities result in greater infiltration flows throughout the flood event.

Q_H begins to develop as soon as river levels start to rise. It peaks early, approximately one day before the start of overbank flooding (t_1), with peak values ranging from 16 m³ s^{-1} in the low-conductivity scenario (SCN25) to 57 m³ s^{-1} in the high-conductivity scenario (SCN27). As the aquifer near the riverbed becomes saturated, Q_H declines due to a reduced hydraulic gradient.

In contrast, Q_V persists for longer and typically peaks during the rising limb of the flood, influenced by the timing and extent of overbank flooding. Q_V continues to enter the aquifer even beyond the flood peak, though with reduced magnitude, and ceases only as water recedes into the main channel. While the timing of the Q_V peak is moderately sensitive to soil hydraulic conductivity, occurring at approximately t_1 + 9 hours in the high-conductivity scenario and at t_1 + 5 days in the low-conductivity case, the duration of the vertical infiltration varies much more substantially between scenarios. Peak Q_V values span an order of magnitude, from 51 m³ s^{-1} (SCN25) to 502 m³ s^{-1} (SCN27).

Figure 5 presents the river-aquifer exchange flow hydrographs at the outlet section of the Tisza River for the three hydraulic conductivity scenarios.

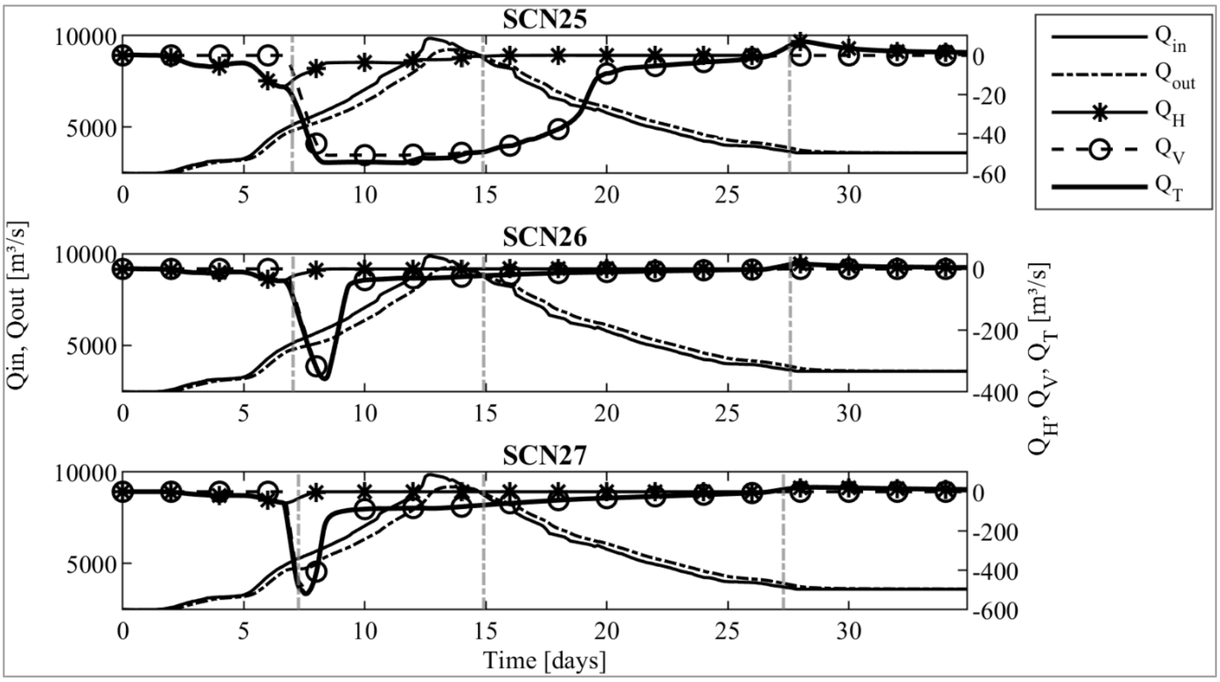

Figure 4. Reach-integrated exchange flow rates between river and aquifer (negative values: flow into the aquifer) for the Lower Danube reach under the conductivity scenarios (SCN25 – low; SCN26 – medium; SCN27 - high). Horizontal exchange flow rate (Q_H) is shown with asterisk markers, vertical exchange flow rate (Q_V) with open-circle markers, and total exchange flow rate ($Q_T = Q_V + Q_H$) with a solid thick line. River discharge at the inflow (Q_{in}) is represented by a solid black line and at the outflow (Q_{out}) by a dash-dot line (Results are shown for a 50 km river reach)

4. ábra. A folyó és a talajvíztartó közötti, az Alsó-Duna 50 km hosszú szakaszára integrált szivárgási vízhozamok (negatív érték: a víztartó felé irányuló áramlás) a különböző hidraulikai vezetőképességi változatok mellett (SCN25 – alacsony; SCN26 – közepes; SCN27 – magas). A vízszintes szivárgási hozamot (Q_H) csillag, a függőlegest (Q_V) üres kör szimbólum jelöli; a kettő összegét ($Q_T = Q_V + Q_H$) vastag folytonos vonal mutatja. A folyó belépő árhullámképét (Q_{in}) fekete folytonos vonal, a kilépőt (Q_{out}) pont-vonal jelzi

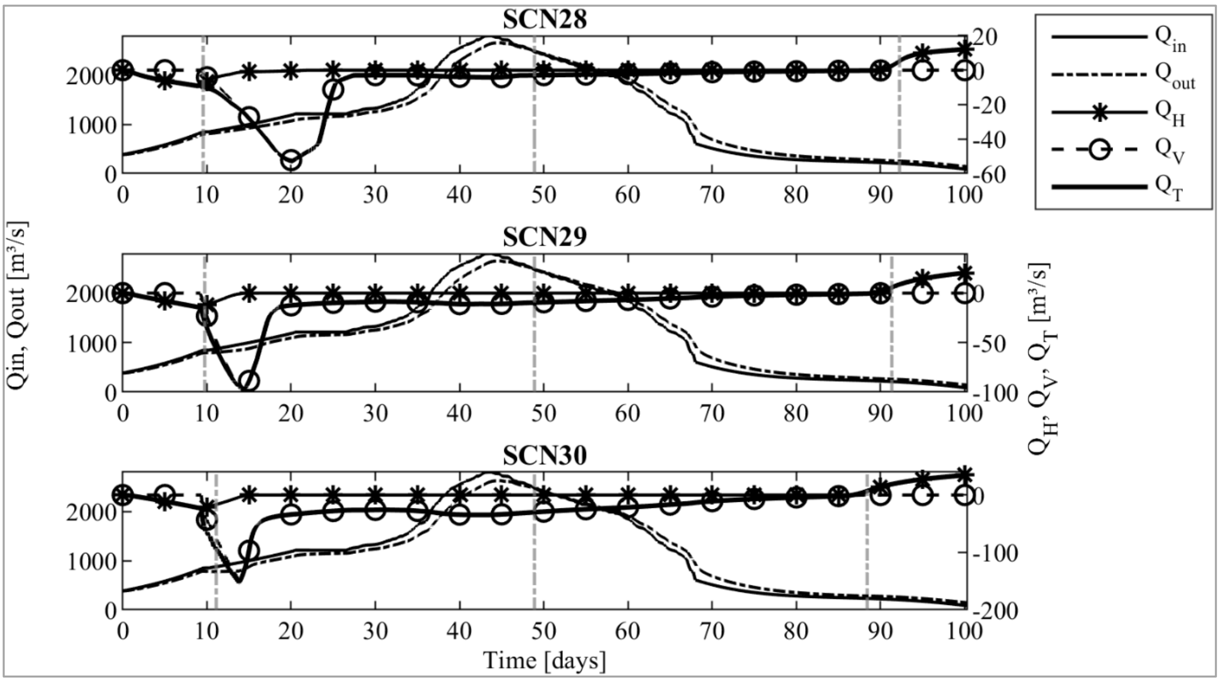

Figure 5. Reach-integrated exchange flow rates between river and aquifer (negative values: flow toward the aquifer) for the Tisza River under the conductivity scenarios (SCN28 – low; SCN29 – medium; SCN30 - high)
(Descriptions of the curves are presented in Figure 4)

5. ábra. A folyó és a víztartó közötti szakaszintegrált szivárgási vízhozamok (negatív érték: a víztartó felé irányuló áramlás) a Tisza folyón a különböző hidraulikai vezetőképességi változatok mellett (SCN28 – alacsony; SCN29 – közepes; SCN30 – magas)
(A görbék jelölése: lásd 4. ábra)

Q_H peaks approximately one day before the onset of overbank flooding (t_1), but the time to peak is sensitive to the hydraulic conductivity, ranging from 14 hours in the low-conductivity scenario (SCN28) to 2 days in the high-conductivity scenarios (SCN30). The peak values of Q_H range from 9 m³ s⁻¹ (SCN28) to 23 m³ s⁻¹ (SCN30).

This is followed by the peaking of Q_V, which occurs on average at t_1 + 6 days, although it varies depending on the scenario. In detail, Q_V peaks at t_1 + 11 days, t_1 + 5 days, and t_1 + 3 days in the low- (SCN28), medium- (SCN29), and high-conductivity (SCN30) scenarios. Peak Q_V values range from 52 m³ s⁻¹ (SCN28) to 150 m³ s⁻¹ (SCN30).

Flood attenuation

To investigate the modification of a flood hydrograph due to bank storage, the inflow hydrograph was routed through a long river reach and evaluated along the uppermost 50 km reach (not impacted by the outflow boundary condition), both with and without infiltration. In the first case, both horizontal and vertical infiltration were allowed through the riverbed and active floodplain, while in the second case, the channel and floodplain were treated as impermeable, preventing any infiltration. *Table 5* summarises the flow and river stage attenuation, as well as flood wave delay, for all simulated scenarios.

The impact of bank storage on flow attenuation is evident across the scenarios. In the Lower Danube simulations, incorporating bank storage resulted in a peak flow reduction of 6.2% (613 m³/s), an excess of +0.5 percentage points (+48 m³/s) compared to the case without infiltration, for the middle scenario (SCN26). Although no delay in peak discharge timing was observed, the inclusion of vertical and horizontal infiltration led to an average decrease in water depth of 3.1 cm in SCN26. In the Tisza River, bank storage reduced the peak flow by 6.2% (151 m³/s), a change of +0.6 percentage points (+16 m³/s) compared to the case without infiltration, for the middle scenario (SCN29). Water levels in the Tisza decreased by 2.8 cm in SCN29. A consistent trend emerges across both rivers: higher soil hydraulic conductivity corresponds with greater flow attenuation, underscoring the effect of permeable soils on the bank storage processes.

During flood events, surface water storage refers to the temporary retention of water within river channels and floodplains, naturally regulating flood wave propagation and peak attenuation. This surface storage was calculated by integrating the channel's wetted cross-sectional area at the local peak flood conditions over the entire modelled reach. When comparing bank storage to total storage (i.e., the sum of surface and bank storage), bank storage contributes a smaller, yet significant, proportion. Its contribution increases with soil permeability: for the Lower Danube, bank storage represents 12%, 16%, and 26% in the low (SCN25) to high (SCN27) conductivity scenarios, respectively. For the Tisza River, the corresponding values are higher: 14%, 21%, and 37% (SCN28 to SCN30).

Table 5. Flow attenuation factor ($\Delta Q/Q_{peak}$) with and without infiltration, river depth attenuation (Δh) with and without infiltration, and time to peak (Δt_{peak}) delay between inflow and outflow with and without infiltration, for all 100-year scenarios
5. táblázat. Relatív vízhozam-csillapítás ($\Delta Q/Q_{peak}$), vízszint-csillapítás (Δh), valamint a tetőzés időeltolása a belépő és kilépő szelvények között (Δt_{peak}) beszivárgással és beszivárgás nélkül, az összes 100 éves árvízi változatra vonatkozóan

Scenario	K_z/m (d⁻¹)	K_x (m/d)	$\Delta Q/Q_{peak}$ w/inf (%)	$\Delta Q/Q_{peak}$ w/out inf (%)	Δt_{peak} w/ inf (h)	Δt_{peak} w/out inf (h)	Δh w/inf (cm)	Δh w/out inf (cm)
Lower Danube	**0.15**	**5**	6.2%	5.7%	17.0	17.0	22.8	19.6
	0.5	**50**	6.2%	5.7%	17.0	17.0	22.7	19.6
	1.5	**500**	6.7%	5.7%	17.0	17.0	25.8	19.6
Tisza	**0.15**	**5**	5.2%	4.8%	25.0	25.0	14.0	12.4
	0.5	**50**	5.4%	4.8%	25.0	25.0	15.1	12.4
	1.5	**500**	6.3%	4.8%	26.0	25.0	18.8	12.4

DISCUSSION

The primary objective of this study was to investigate infiltration into the aquifer during extreme (100-year) flood events, with a focus on how different combinations of river, aquifer, and flood hydrograph characteristics affect river-aquifer exchange and contribute to flood attenuation. The analysis centred on the two major Hungarian rivers, the Danube River and the Tisza River, which represent two distinct river configurations with large levee-protected floodplains where accurate prediction of flood attenuation is critical.

A prismatic, symmetric river geometry was adopted and evaluated against observed flow rates and overbank depths derived from hydraulic modelling based on surface water gauge data. The transferability of the calibrated model parameters was then assessed by applying them to a different reach of the Danube River. This comparison showed that the simplified geometry provides a reasonable representation for scenario-based sensitivity analyses.

To assess the influence of soil hydraulic properties, multiple scenarios were tested for each river, varying both horizontal and vertical (floodplain surface layer) conductivity values. Calibration was performed using groundwater observations from the 2013 flood in the Lower Danube Reach. The modelled bank storage estimates aligned well with observational data under the medium-conductivity scenario, confirming the model's capability to realistically simulate infiltration-driven bank storage during major flood events.

For lowland rivers such as the Hungarian reaches of the Lower Danube and Tisza, both horizontal (Q_H) and vertical (Q_V) reach-integrated infiltration flow rates tended to peak during the rising limb of the flood. Q_H declined rapidly as the hydraulic gradient decreased and the floodplain became progressively saturated, whereas Q_V persisted longer, remaining active through much of the rising limb of the hydrograph.

The timing and magnitude of these peaks were strongly influenced by soil hydraulic conductivity: in high-conductivity scenarios, infiltration rates peaked quickly and reached higher values, while in low-conductivity scenarios, the peaks were lower but more sustained. This pattern is consistent with the findings of *Helton et al. (2014)* and *Doble et al. (2012)*, who reported that aquifer exchange is initially high as floodwaters spread across the floodplain and then diminishes as sediments saturate and the river stage increases.

Mean river–aquifer exchange flows were higher in the Lower Danube River, driven by steeper hydraulic gradients and rapid rates of overbank water level rise (~47 cm/day), compared to ~8 cm/day for the Tisza. However, the Tisza River exhibited much greater total bank storage volumes, attributed primarily to its longer inundation duration and secondarily to its wider floodplain. Vertical infiltration through the active floodplain dominated bank storage in both rivers: 90% in the Danube and 91% in the Tisza. These values are consistent with *Bernard-Jannin et al. (2016)*, who reported 88% floodplain infiltration in the Garonne River (Spain), reinforcing the importance of surface water–groundwater exchange through overbank flows in flood modelling.

Over a 50 km reach, the Lower Danube showed an average flow peak reduction of 6.4% (Tisza: 5.6%) and a peak water level decrease of 4 cm (Tisza: 6.4 cm). Our results show that bank storage contributed significantly to this attenuation, reducing flows and water levels in both systems and accounting for 12–26% of total storage in the Danube and 14–37% in the Tisza. The Danube River's rapid rise produced higher infiltration flow rates, aligning with findings by *Hou et al. (2021),* which noted that a rapid rise in flood depth enhances infiltration by inundating more land earlier in the flood event. *Ubell (1963)* similarly highlighted that infiltration is influenced not only by the hydraulic gradient but also by the intensity of river level fluctuations, with rapid surface water rises promoting higher infiltration rates. Yet, despite these elevated exchange flow rates in the Danube, the Tisza River's longer inundation and broader floodplain enabled more sustained infiltration and greater peak reduction. This shows that the duration and spatial extent of flooding can be more influential than the exchange flow rates alone.

While often underrepresented in flood models, bank storage has been shown in this study to play a substantial role in water retention and flood attenuation. To improve model accuracy and efficiency, especially in flood risk mapping and flood forecasting, incorporating infiltration and bank storage effects is essential (*Szilagyi 2004, Hou et al. 2021*). Even when the model's process description doesn't represent bank storage, the resulting errors are partly mitigated during the calibration of the flow resistance parameters (e.g., Manning's n), by matching peak river water levels, peak river discharges and flood propagation speed. However, this compensation remains imperfect because roughness and bank storage influence flood dynamics through different mechanisms. Roughness mainly affects momentum losses and flood-wave routing, whereas bank storage introduces temporary subsurface storage and delayed groundwater release, acting over longer timescales than surface storage processes. Consequently, calibration of roughness parameters cannot fully reproduce the temporal shift associated with groundwater storage and release.

This limitation becomes increasingly important when models are extrapolated beyond the flood events used for calibration. In the present study, neglecting infiltration reduced the average attenuation in the Danube from 6.4% to 5.7% for the analysed 100-year flood scenarios. For the Tisza River, attenuation decreased from 5.6% to 4.8%. Although the attenuation differences are comparable between both rivers, bank storage was considerably larger in the Tisza due to its wider floodplain and longer flood duration. In addition, the sensitivity to hydraulic conductivity was more pronounced in the Tisza, where the variation among permeability scenarios was approximately twice that observed for the Danube. These findings indicate that roughness calibration may reproduce observed flood levels within the calibration range, but may become less reliable when applied to flood events with different magnitudes, durations, or floodplain inundation extents, where infiltration and groundwater storage processes play a larger role.

Sedimentation can reduce soil permeability (as well as surface storage) over time. In particular, in the Middle and Lower Tisza River, sedimentation rates of 1.1 cm yr^{-1} and 0.8 cm yr^{-1}, respectively, have led to rising riverbed levels (*Murányi and Koncsos 2022*), which in turn reduce hydraulic conductivity and limit bank storage. These authors also explore the reconnection of deep floodplains along the Tisza to increase surface storage by up to 2400 million m^3. In addition to this storage, our study shows that, for a 100-year flood, subsurface storage may represent 14–37% of surface storage in the Middle Tisza River, increasing the relevance of adding river-aquifer interactions when studying alternative nature-based solutions for flood risk mitigation. It is worth noting that bank storage over a 50 km river reach is of the same order of magnitude as the storage capacity of existing or planned flood retention reservoirs on the middle reach of the Tisza River (Tiszaroffi: 97, Hanyi-Tiszasülyi: 247, Nagykunsági: 99 million m^3) (*Ungvári and Kis 2021*). Similarly, *Schweitzer (2015)* reported a trend of flood wave heights rising by 2–3 cm yr^{-1} along the Tisza River between 1970 and 2013 due to channel capacity deterioration.

In the present modelling framework, the riverbed leakance factor (K_{rb}/m_{rb}) was assumed constant across all scenarios in order to isolate the influence of aquifer hydraulic conductivity and floodplain vertical leakance on bank storage dynamics. However, sedimentation processes may modify the permeability of the riverbed and create clogging layers that reduce hydraulic connectivity between the river and aquifer. Future work could therefore explore the sensitivity of river-aquifer exchange flows to variations in riverbed leakance, particularly in systems where sediment accumulation progressively alters riverbed hydraulic properties.

Finally, our simulations reveal that in both the Lower Danube and Tisza rivers, bank storage extended well beyond the active floodplain in the medium- to high-conductivity scenarios, reaching a distance of 1–3 km from the levee. This has negative implications for flood control infrastructure, since prolonged flood waves have historically led to dike breaches on the Tisza (*Lóczy 2010*), especially when subsurface flow pressures build up. Hence, flood mitigation strategies should carefully balance structural measures with natural processes such as infiltration and groundwater recharge.

CONCLUSIONS

This study investigated river–aquifer interactions during extreme flood events in two lowland river reaches, approximating the Lower Danube River and the Middle Tisza River in Hungary, using a physically based modelling approach. By simulating a range of infiltration scenarios across varying soil hydraulic conductivities, we assessed the role of bank storage in flood dynamics.

Our results demonstrate that bank storage is a significant component of total floodwater storage, accounting for up to 26% in the Lower Danube and up to 37% in the Tisza, particularly assuming a highly conductive aquifer. While the Danube River exhibited higher mean infiltration flow rates, driven by a steep hydraulic gradient and rapid overbank rise, the Tisza River showed greater bank storage and stronger attenuation of the river flood wave. This is attributed primarily to its longer flood durations, which allow for more extensive and sustained infiltration.

These findings underscore the benefits of accounting for bank storage in flood modelling and flood risk assessment. Incorporating infiltration dynamics improves predictions of flood peak magnitudes and durations. From a management perspective, recognizing the contribution of subsurface storage can support nature-based flood mitigation strategies, such as floodplain reconnection, or dike relocation with better (increased) estimates of storage capacity.

ACKNOWLEDGEMENTS

This research was funded by the Ministry of Culture and Innovation and the National Research, Development and Innovation Office under Grant Nr. TKP2021-NVA-02. Furthermore, this work was carried out as part of the first author's studies supported by the Stipendium Hungaricum Scholarship through the Hungarian Government's initiative, administered via the Tempus Public Foundation; the author thanks the programme for the opportunity.

REFERENCES

Bernard-Jannin, L., Brito, D., Sun, X., Jauch, E., Neves, R., Sauvage, S., Sánchez-Pérez, J. M. (2016). Spatially distributed modelling of surface water-groundwater exchanges during overbank flood events-a case study at the Garonne River. Advances in Water Resources, 94, pp. 146-159. https://doi.org/10.1016/j.advwatres.2016.05.008

Brunner, P., Cook, P.G, Simmons, C.T. (2009). Hydrogeologic controls on disconnection between surface water and groundwater, Water Resour. Res., 45, W01422. https://doi.org/10.1029/2008WR006953

Derx, J., Blaschke, A.P., Blöschl, G. (2010). Three-dimensional flow patterns at the river-aquifer interface: A case study at the Danube. Advances in Water Resources, 33(11), pp. 1375-1387. https://doi.org/10.1016/j.advwatres.2010.04.013

Doble, R.C., Crosbie, R.S., Smerdon, B.D., Peeters, L., Cook, F.J. (2012). Groundwater recharge from overbank floods. Water Resources Research, 48(9), W09522. https://doi.org/10.1029/2011WR011441.

Harbaugh, A.W. (2005). MODFLOW-2005, the US Geological Survey modular ground-water model: the ground-water flow process (Vol. 6). Reston, VA, USA: US Department of the Interior, US Geological Survey. https://doi.org/10.3133/tm6A16

Helton, A.M., Poole, G.C., Payn, R.A., Izurieta, C., Stanford, J.A. (2014). Relative influences of the river channel, floodplain surface, and alluvial aquifer on simulated hydrologic residence time in a montane river floodplain. Geomorphology, 205, pp. 17-26. https://doi.org/10.1016/j.geomorph.2012.01.004

Hong, M., Mohanty, B.P., Sheng, Z. (2020). An explicit scheme to represent the bidirectional hydrologic exchanges between the vadose zone, phreatic aquifer, and river. Water Resources Research, 56(9), e2020WR027571. https://doi.org/10.1029/2020WR027571.

Hou, J., Zhang, Z., Zhang, D., Shi, B., Chen, G., Zhang, H. (2021). Study on the influence of infiltration on flood propagation with different peak shape coefficients and duration. Water Policy, 23(4), pp. 1059-1074. https://doi.org/10.2166/wp.2021.193

Kolencsik-Tóth, A., Kovács, B. (2015). Calibration process for groundwater flow model of a river influenced shallow aquifer. Central European Geology, 58(1-2), pp. 186-198. https://doi.org/10.1556/24.58.2015.1-2.12

Krause, S., Bronstert, A., Zehe, E. (2007). Groundwater-surface water interactions in a North German lowland floodplain: Implications for the river discharge dynamics and riparian water balance. Journal of Hydrology, 347(3-4), pp. 404-417. https://doi.org/10.1016/j.jhydrol.2007.09.028

Li, Y., Yao, J., Zhao, G., Zhang, Q. (2017). Evidences of hydraulic relationships between groundwater and lake water across the large floodplain wetland of Poyang Lake, China. Water Science and Technology: Water Supply, 18(2), pp. 698-712. https://doi.org/10.2166/ws.2017.150

Liang, X., Zhan, H., Schilling, K. (2018). Spatiotemporal responses of groundwater flow and aquifer-river exchanges to flood events. Water Resources Research, 54(3), pp. 1513-1532. https://doi.org/10.1002/2017WR022046.

Lóczy, D. (2010). Flood hazard in Hungary: A re-assessment. Central European Journal of Geosciences, 2, pp. 537-547.https://doi.org/10.2478/v10085-010-0029-0.

Murányi, G., Koncsos, L. (2022). Analysis of nature-based flood management in the Tisza River Valley, Hungary. Pollack Periodica.
https://doi.org/10.1556/606.2022.00456

Murinkó, G., Bene, K. (2017). Hydrologic modelling of the loess bluff in Dunaujvaros, Hungary. Pollack Periodica, 12(1), pp. 3-15.
https://doi.org/10.1556/606.2017.12.1.1

Nguyen, W.D., Datta, S., Knappett, P.S., Cardenas, M.B. (2025). The Effects of Tidal and Seasonal Scale Flooding and Soil Texture on Surface Water-Groundwater Interactions Along a Fluvio-Deltaic Floodplain: The Meghna River, Bangladesh. Water Resources Research, 61(10), e2025WR039919.
https://doi.org/10.1029/2025WR039919.

Pinder, G.F., Sauer, S. P. (1971). Numerical simulation of flood wave modification due to bank storage effects. Water Resources Research, 7(1), pp. 1-25. https://doi.org/10.1029/WR007i001p00063

Saksena, S., Merwade, V., Singhofen, P.J. (2019). Flood inundation modelling and mapping by integrating surface and subsurface hydrology with river hydrodynamics. Journal of Hydrology, 575, pp. 1155-1177. https://doi.org/10.1016/j.jhydrol.2019.06.024

Schweitzer, F. (2015). Strategy or disaster: New-style river regulation as an issue of national security. Hungarian Geographical Bulletin, 64(4), pp. 307-315. https://doi.org/10.15201/hungeobull.64.4.5

Shuai, P., Knappett, P.S., Hossain, S., Hosain, A., Rhodes, K., Ahmed, K.M., Cardenas, M.B. (2017). The impact of the degree of aquifer confinement and anisotropy on tidal pulse propagation. Groundwater, 55(4), pp. 519-531. https://doi.org/10.1111/gwat.12509

Sophocleous, M. (2002). Interactions between groundwater and surface water: the state of the science. Hydrogeology Journal, 10, pp. 52-67.
https://doi.org/10.1007/s10040-001-0170-8

Szilagyi, J. (2004). Accounting for stream-aquifer interactions in the state-space discretization of the Kalinin-Milyukov-Nash cascade for streamflow forecasting. Journal of Hydrologic Engineering, 9(2), pp. 135-143. https://doi.org/10.1061/(ASCE)1084-0699(2004)9:2(135)

Trásy, B., Magyar, N., Havril, T., Kovács, J., Garamhegyi, T. (2020). The Role of Environmental Background Processes in Determining Groundwater Level Variability-An Investigation of a Record Flood Event Using Dynamic Factor Analysis. Water, 12(9), 2336.
https://doi.org/10.3390/w12092336

Ubell, K. (1963). Surface-and groundwater relationships along the Hungarian reach of the Danube River. In Symposium surface waters held at the occasion of general assembly of Berkeley of IUGG, Vol. 19, No. 31.8.

Ubell K. (1964). A folyó és talajvíz összefüggése a Duna mentén [The relationship between the river and groundwater along the Danube]. Hidrológiai Közlöny, 44(5), pp. 193–200.

Ungvári, G., Kis, A. (2022). Reducing flood risk by effective use of flood-peak polders: A case study of the Tisza River. Journal of Flood Risk Management, 15(3), e12823. https://doi.org/10.1111/jfr3.12823

Vivoni, E.R., Bowman, R.S., Wyckoff, R.L., Jakubowski, R.T., Richards, K.E. (2006). Analysis of a monsoon flood event in an ephemeral tributary and its downstream hydrologic effects. Water Resources Research, 42(3). https://doi.org/10.1029/2005WR004036

Wagner F., Csoma R. (2022). A felszín alatti áramlás és árhullámok kapcsolatának vizsgálata változó folyami vízszintek esetében. Hidrológiai Közlöny, 102(3), pp. 50-60.

Weng, P., Sánchez-Pérez, J.M., Sauvage, S., Vervier, P., Giraud, F. (2003). Assessment of the quantitative and qualitative buffer function of an alluvial wetland: Hydrological modelling of a large floodplain (Garonne River, France). Hydrological Processes, 17(12), pp. 2375-2392. https://doi.org/10.1002/hyp.1248

Zitta, V.L., Wiggert, J.M. (1971). Flood routing in channels with bank seepage. Water Resources Research, 7(5), pp. 1341-1345.
https://doi.org/10.1029/WR007i005p01341.

AUTHORS

GADADHARA FERRAZ is a hydraulic engineer. She obtained her master's degree in Environmental technology and Water resources at the Federal University of Pernambuco, Brazil, in 2019. She is currently a Ph.D. candidate in Hydraulics and Water Resources at the Budapest University of Technology and Economics, Hungary. Her research focuses on river–aquifer interactions, and their role in flood dynamics.

TAMÁS KRÁMER obtained his Ph.D. in civil engineering in 2007, and is currently an associate professor at Budapest University of Technology and Economics (BME). His research is focused on the hydrodynamics of surface waters, with an emphasis on rivers, lakes and floodplains. He introduced methodological innovations and contributed to flood protection and flood forecasting, and his research results support major projects on the country's largest lakes. He has been a member of the Hungarian Hydrological Society since 2000.